ACADEMIC PRESS

Available online at www.sciencedirect.com

SCIENCE DIRECT®

Journal of Magnetic Resonance 163 (2003) 236–247

JMR Journal of Magnetic Resonance

www.elsevier.com/locate/jmr

Gaussian approximation in the theory of MR signal formation in the presence of structure-specific magnetic field inhomogeneities

Alexander L. Sukstanskii* and Dmitriy A. Yablonskiy

Biomedical MR Lab, Mallinckrodt Institute of Radiology, Washington University, St. Louis, MO 63110, USA

Received 27 December 2002; revised 25 March 2003

Abstract

A detailed theoretical analysis of the free induction decay (FID) and spin echo (SE) MR signal formation in the presence of mesoscopic structure-specific magnetic field inhomogeneities is developed in the framework of the Gaussian phase distribution approximation. The theory takes into account diffusion of nuclear spins in inhomogeneous magnetic fields created by arbitrarily shaped magnetized objects with permeable boundaries. In the short-time limit the FID signal decays quadratically with time and depends on the objects' geometry only through the volume fraction, whereas the SE signal decays as 5/2 power of time with the coefficient depending on both the volume fraction of the magnetized objects and their surface-to-volume ratio. In the motional narrowing regime, the FID and SE signals for objects of finite size decay mono-exponentially; a simple general expression is obtained for the relaxation rate constant ΔR_2. In the case of infinitely long cylinders in the motional narrowing regime the theory predicts non-exponential signal decay $\ln S \sim -t \ln t$ in accordance with previous results. For specific geometries of the objects (spheres and infinitely long cylinders) exact analytical expressions for the FID and SE signals are given. The theory can be applied, for instance, to biological systems where mesoscopic magnetic field inhomogeneities are induced by deoxygenated red blood cells, capillary network, contrast agents, etc.

Keywords: Magnetic resonance; Relaxation effects; fMRI

1. Introduction

Magnetic field inhomogeneities are known to play a significant role in the process of magnetic resonance signal formation. Inhomogeneities of mesoscopic scale (smaller than a voxel size but bigger than the atomic scale) originating from internal, structure-specific sources could provide important information on biological tissue structure and function. These mesoscopic inhomogeneities result from the differences in magnetic susceptibility within a biological system. Examples include deoxygenated red blood cells, capillary network, contrast agents for MRI, and so on. Usually such systems are described in the framework of a model, according to which the magnetized objects (blood vessels, red blood cells, etc.) occupying a volume fraction ζ with a magnetic susceptibility χ_i are embedded in a given media with a magnetic susceptibility χ_e. Nuclear spins in the non-uniform magnetic field induced by these objects precess with spatially dependent Larmor frequencies and accumulate different phases, leading to signal decay. Spin diffusion plays two major roles: on the one hand, it smears phase differences; on the other hand it makes impossible complete spin phase refocusing in spin echo (SE) experiments. In the static dephasing (or slow motion) regime, after an RF excitation pulse, the MR signal decays due to phase differences faster than spins average out their phases due to diffusion. In the motional narrowing (fast diffusion) regime, phase averaging is the fastest process defining MR signal relaxation, and the rate of the latter is inversely proportional to the diffusion coefficient of the spins.

Substantial insights into understanding details of MR signal formation in the presence of mesoscopic field inhomogeneities came from Monte–Carlo simulation [1–5] and analytical approaches that described MR signal in limiting cases of slow motion and motional narrowing

* Corresponding author. Fax: 1-314-362-0526.
E-mail address: alex@wuchem.wustl.edu (A.L. Sukstanskii).

1090-7807/$ - see front matter © 2003 Elsevier Science (USA). All rights reserved.
doi:10.1016/S1090-7807(03)00131-9

regimes [6–12]. A rather attractive approach has been proposed by Kennan et al. [13] and further developed by Stables et al. [14], where simple analytical equations were suggested to describe MR signal in all regimes. This approach was based on a Gaussian approximation for the spin-phase distribution function and an additional assumption of a mono-exponentially decaying frequency correlation function similar to that in the Anderson–Weiss mean field theory [15]. Such a behavior of the correlation function can be expected for diffusion inside bounded volumes because a solution to the diffusion equation in these cases can be represented as a sum of eigenfunctions with *discrete* positive eigenvalues and the dominant role of the smallest eigenvalue can lead to a mono-exponential time dependence of the correlation function. In the case of unrestricted diffusion, the set of eigenvalues is *continuous*; hence, the correlation function can be non-exponential. Indeed, if magnetic field inhomogeneities are created by magnetized spheres embedded in a homogeneous medium, Jensen and Chandra [10] demonstrated that the correlation function time dependence is not exponential but algebraic. In the present paper, we calculate the frequency correlation function for objects of arbitrary geometry and apply it to develop a Gaussian-based theory of MR signal formation.

The Gaussian approach was first proposed by Douglass and McCall [16] for an analysis of MR signal in the presence of a constant field gradient for the case of unrestricted diffusion when it represents an exact solution to the problem. If diffusion is restricted by some barriers or if the field gradients are non-uniform (as in the case of susceptibility-induced field inhomogeneities), the phase distribution function is, in general, not Gaussian. An adequateness of the Gaussian approximation was discussed by many authors (see, e.g. [17–20]). A detailed quantitative comparison of the Gaussian approximation with exact results obtained in the framework of the random walk approach for some models of restricted diffusion in the presence of a constant field gradient was given in [21] for a broad range of the system parameters. It was demonstrated that for a SE signal this approximation is adequate for the description of MR signals corresponding to arbitrary system parameters—the maximum discrepancy between an exact SE signal and that from the Gaussian approximation does not exceed several percent while the signal decays to $1/e$ of its initial value. For the free induction decay (FID) signal, the Gaussian approximation is shown to be an adequate in the motional narrowing regime and for short times. In the problem of susceptibility-induced magnetic inhomogeneities, we can also expect that the Gaussian approach will be adequate under the same conditions.

In the present paper, the Gaussian approximation is applied to analysis of the FID and SE signals in the model with magnetized objects of arbitrary geometry. We consider that: (A) the volume fraction occupied by the objects is small; and (B) diffusion is unrestricted and spins freely penetrate inside the objects, where they diffuse with the same diffusion coefficient as outside. Systems containing objects with impermeable boundaries will be discussed separately.

In what follows, we will obtain rather simple expressions describing the FID and SE signals in the presence of uniformly distributed and uniformly oriented magnetized objects of arbitrary geometry. In particular, we will show that a mean value of ω^2 ($\omega = \gamma H(\mathbf{r})$) is the Larmor frequency in the rotating frame, $H(\mathbf{r})$ is the local inhomogeneous magnetic field induced by magnetized objects, and γ is the gyromagnetic ratio) does not depend on objects' geometry but is determined only by the volume fraction ζ and a susceptibility difference $\Delta\chi = \chi_i - \chi_e$:

$$\langle \omega^2 \rangle = \frac{4\zeta(\delta\omega_s)^2}{45}, \tag{1}$$

where $\delta\omega_s = 4\pi \cdot \Delta\chi \cdot \gamma \cdot H_0$, and H_0 is the external magnetic field. The short-time behavior of the FID signal is also independent of objects' geometry

$$S_{\mathrm{FID}}(t) \simeq S_0 \cdot \exp\left[-\frac{2\zeta(\delta\omega_s)^2}{45} t^2\right], \tag{2}$$

where S_0 describes the signal in the absence of the magnetic inhomogeneities. The SE short-time behavior depends on the objects' volume fraction and also on their geometry through the surface-to-volume ratio s_0/v_0,

$$S_{\mathrm{SE}}(t) \simeq S_0 \cdot \exp\left[-\frac{8(\sqrt{2}-1)\zeta(\delta\omega_s)^2}{675} \frac{s_0}{v_0} \left(\frac{2D}{\pi}\right)^{1/2} t^{5/2}\right]. \tag{3}$$

We note the unusual $t^{5/2}$ time dependence of the SE signal instead of the t^3 dependence in the case of impenetrable objects. The long-time asymptotic behavior of the FID and SE signals in the motional narrowing regime is mono-exponential and can be described by a standard ΔR_2 (or ΔR_2^* for FID) relaxation rate

$$\Delta R_2 \simeq \Delta R_2^* \simeq \frac{\zeta(\delta\omega_s)^2}{45\pi D v_0} \cdot \int\int_{v_0} \frac{d\mathbf{r}_1\, d\mathbf{r}_2}{|\mathbf{r}_1 - \mathbf{r}_2|}, \tag{4}$$

where integration is only over one object's volume, provided that the integral in (4) exists. An important exception when the integral in Eq. (4) does not exist is the case of infinitely long cylinders; in this case, the signal decays non-mono-exponentially (see Eq. (42)).

2. General approach

In the general case, the MR signal produced by a system of a large number of spins, freely diffusing and precessing in magnetic field, at time t after an RF pulse is

$$S(t) = S_0 \cdot s(t), \quad s(t) = \langle \exp[\mathrm{i}\varphi(t)] \rangle, \tag{5}$$

where the factor S_0 describes the signal in the absence of magnetic field inhomogeneities and $\varphi(t)$ is the phase accumulated by a single spin moving along a given trajectory $\mathbf{r} = \mathbf{r}(t)$ by time t

$$\varphi(t) = \int_0^t \mathrm{d}t' \omega(\mathbf{r}(t')). \tag{6}$$

In Eq. (6) the Larmor frequency $\omega(\mathbf{r}(t)) = \gamma H(\mathbf{r}(t))$, where $H(\mathbf{r}(t))$ includes the magnetic field created by all magnetized objects on a spin trajectory $\mathbf{r}(t)$. The angular brackets in Eq. (5) mean averaging over all possible initial positions and trajectories of the diffusing spins. Additionally, if magnetic field inhomogeneities are induced by uniformly distributed and uniformly oriented magnetized objects, $\langle \cdots \rangle$ includes also averaging over possible positions and orientations of the objects. Thus,

$$\langle \cdots \rangle \equiv \langle \cdots \rangle_{\text{diffusion+position+orientation}}. \tag{7}$$

Introducing a phase distribution function $P(\varphi, t)$, the signal in Eq. (5) can be written as

$$s(t) = \int_{-\infty}^{\infty} \mathrm{d}\varphi \, P(\varphi, t) \exp(\mathrm{i}\varphi) \tag{8}$$

(hereafter the function $s(t)$ will be referred to as the "signal"). In the Gaussian approximation

$$P(\varphi, t) = \frac{1}{(2\pi\langle\varphi^2(t)\rangle)^{1/2}} \exp\left[-\frac{\varphi^2}{2\langle\varphi^2(t)\rangle}\right]. \tag{9}$$

Without loss of generality, we consider $\langle\varphi\rangle = 0$. In this case, the signal can be reduced to

$$s(t) = \exp\left[-\frac{1}{2}\langle\varphi^2(t)\rangle\right]. \tag{10}$$

Averaging $\varphi^2(t)$ rather than the exponent $\exp(i\varphi)$ in Eq. (5) is required in this approach, that is a substantially less challenging problem.

In the framework of the Gaussian approximation, the FID signal (experiment with a single broadband 90° RF pulse followed by a readout period t) and the SE signal (experiment with $90° - t/2$–$180° - t/2$ RF pulses) can be written from Eq. (10) in the form:

$$s(t) = \exp[-\Gamma(t)], \quad \Gamma_{\mathrm{FID}}(t) = \int_0^t \mathrm{d}t_1 \int_0^{t_1} \mathrm{d}t_2 G(t_1, t_2),$$
$$\Gamma_{\mathrm{SE}}(t) = \left[\int_0^t \mathrm{d}t_1 \int_0^{t_1} \mathrm{d}t_2 - 2 \cdot \int_{t/2}^t \mathrm{d}t_1 \int_0^{t/2} \mathrm{d}t_2\right] G(t_1, t_2), \tag{11}$$

where $G(t_1, t_2)$ is the frequency correlation function,

$$G(t_1, t_2) = \langle \omega(t_1)\omega(t_2) \rangle_{\text{diffusion+position+orientation}}. \tag{12}$$

In what follows, the function $\Gamma(t)$ will be referred to as the signal attenuation function.

Diffusion averaging in Eq. (12) over all possible spin trajectories and initial positions can be done in a standard manner by introducing an initial spin distribution $\rho(\mathbf{r}_0)$ and the propagator $P(\mathbf{r}_1, \mathbf{r}_2, t)$ defining the probability for a spin to diffuse from a point $\mathbf{r}_2$ to a point $\mathbf{r}_1$ during time t

$$\langle \omega(t_1)\omega(t_2) \rangle_{\text{diffusion}} = \int\int\int \mathrm{d}\mathbf{r}_0 \, \mathrm{d}\mathbf{r}_1 \, \mathrm{d}\mathbf{r}_2 \rho(\mathbf{r}_0)\omega(\mathbf{r}_1)\omega(\mathbf{r}_2) \times P(\mathbf{r}_2, \mathbf{r}_0, t_2) P(\mathbf{r}_1, \mathbf{r}_2, t_1 - t_2), \tag{13}$$

where the integration is over a system volume V. The propagator $P(\mathbf{r}_1, \mathbf{r}_2, t)$ satisfies the diffusion equation

$$\partial P/\partial t = D \cdot \nabla^2 P \tag{14}$$

with the initial condition $P(\mathbf{r}_1, \mathbf{r}_2, 0) = \delta(\mathbf{r}_1 - \mathbf{r}_2)$. For unrestricted diffusion (as assumed throughout this work) the solution to this equation is well-known

$$P(\mathbf{r}_1, \mathbf{r}_2, t) = \frac{1}{(4\pi Dt)^{3/2}} \exp\left[-\frac{(\mathbf{r}_1 - \mathbf{r}_2)^2}{4Dt}\right]. \tag{15}$$

In the case of a uniform initial spin distribution, $\rho(\mathbf{r}_0) = 1/V$, the correlation function G turns out to be a function of the time difference $t = t_1 - t_2$ only:

$$G(t) = \frac{1}{V}\left\langle \int\int \mathrm{d}\mathbf{r}_1 \, \mathrm{d}\mathbf{r}_2 \omega(\mathbf{r}_1)\omega \times (\mathbf{r}_2) P(\mathbf{r}_1, \mathbf{r}_2, t) \right\rangle_{\text{position+orientation}}, \tag{16}$$

and Eqs. (11) for the signal attenuation function $\Gamma(t)$ can be simplified as

$$\Gamma_{\mathrm{FID}}(t) = \int_0^t \mathrm{d}\tau (t - \tau) G(\tau),$$
$$\Gamma_{\mathrm{SE}}(t) = \int_0^t \mathrm{d}\tau (t - \tau)[G(\tau/2) - G(\tau)]. \tag{17}$$

As shown in Appendix A, averaging over positions and orientations of the magnetized objects results in the following expression for the correlation function:

$$G(t) = \frac{G_0}{v_0} \cdot \int\int_{v_0} \mathrm{d}\mathbf{r}_1 \, \mathrm{d}\mathbf{r}_2 P(\mathbf{r}_1, \mathbf{r}_2, t) = \frac{G_0}{v_0 (4\pi Dt)^{3/2}} \cdot \int\int_{v_0} \mathrm{d}\mathbf{r}_1 \, \mathrm{d}\mathbf{r}_2 \exp\left[-\frac{(\mathbf{r}_1 - \mathbf{r}_2)^2}{4Dt}\right], \tag{18}$$

where an integration is over a single object's volume only. The factor G_0 is

$$G_0 = G(0) = \frac{4\zeta(\delta\omega_s)^2}{45}. \tag{19}$$

It is important to emphasize that Eq. (18), in spite of its simple form, takes into account the real distribution of the inhomogeneous magnetic field created by the objects of arbitrary geometry. This fact substantially facilitates the problem of calculating the correlation function because explicit analytical expressions for the local magnetic field $h(\mathbf{r})$ (or its Fourier transformation) are available only for some simplest object geometries. Besides, even in a comparably simple case of ellipsoids of revolution, the expression for $h(\mathbf{r})$ is rather cumbersome [22].

It should be noted that, according to Eq. (16), the quantity $G(0)$ is equal to $\langle\omega^2\rangle$ and the result (19) means that the average value of the square of the Larmor frequency given in Eq. (1) is determined only by the volume fraction ζ and the susceptibility difference $\Delta\chi$ and is independent of the geometry of the objects.

Substituting Eq. (18) in Eqs. (17), we obtain for the signal attenuation function $\Gamma(t)$:

$$\Gamma(t) = \frac{\zeta(\delta\omega_s)^2}{180D^2\pi v_0}\cdot\int\int_{v_0} d\mathbf{r}_1\, d\mathbf{r}_2 |\mathbf{r}|\cdot U\left(\frac{Dt}{r^2}\right), \tag{20}$$

where $r = |\mathbf{r}| = |\mathbf{r}_1 - \mathbf{r}_2|$ and the function $U(x)$ is given by

$$\begin{aligned} U_{\mathrm{FID}}(x) &= 2(2x+1)\tilde{\Phi}\left(\frac{1}{2x^{1/2}}\right) - 4\left(\frac{x}{\pi}\right)^{1/2}\exp\left(-\frac{1}{4x}\right),\\ U_{\mathrm{SE}}(x) &= 2\left[4(x+1)\tilde{\Phi}\left(\frac{1}{(2x)^{1/2}}\right) - (2x+1)\tilde{\Phi}\left(\frac{1}{2x^{1/2}}\right)\right]\\ &\quad + 4\left(\frac{x}{\pi}\right)^{1/2}\left[\exp\left(-\frac{1}{4x}\right) - 2^{3/2}\exp\left(-\frac{1}{2x}\right)\right]. \end{aligned} \tag{21}$$

Here $\tilde{\Phi}(x) = 1 - \Phi(x)$, $\Phi(x)$, and $\tilde{\Phi}(x)$ are the error function and complementary error function [23], respectively. For large x, $x \gg 1$, both the functions $U_{\mathrm{FID}}(x)$ and $U_{\mathrm{SE}}(x)$ are linear in x,

$$U_{\mathrm{FID}}(x) \simeq U_{\mathrm{SE}}(x) \simeq 4x. \tag{22}$$

For small arguments, both of the functions tend to zero non-analytically: $U_{\mathrm{FID,SE}}(x) \sim x^{3/2}\exp(-1/4x)$.

2.1. Long-time limit

In the long-time limit, when $t \gg t_D$, $t_D = R^2/D$ is the characteristic time for diffusion over a characteristic size of the object R, the integrand in Eq. (18) is about 1 for any $\mathbf{r}_1$ and $\mathbf{r}_2$, and for the correlation function $G(\tau)$ we obtain an asymptotic expression

$$G(t) \simeq G_0\frac{v_0}{(4\pi Dt)^{3/2}} \sim t^{-3/2}, \quad t \gg t_D. \tag{23}$$

Note that Eq. (23) is valid only for finite objects; if one of the object's dimensions is infinite then this asymptotic behavior becomes inadequate. For example, for infinitely long cylinders, for an arbitrary long time t, there are some coordinates $\mathbf{r}_1$ and $\mathbf{r}_2$ in the integral in Eq. (18), for which the parameter $(\mathbf{r}_1 - \mathbf{r}_2)^2/Dt$ is not small. In this case, however, one can easily perform the integration over the cylinder axis and obtain the result characteristic to two-dimensional diffusion

$$G(t) \simeq G_0\frac{R^2}{4Dt} \sim t^{-1}, \quad t \gg t_D, \tag{24}$$

where R is the cylinder radius. This result should be expected because the magnetic field created by an infinite cylinder is homogeneous along its axis and therefore spin diffusion in such a field can be treated as two-dimensional.

In the limit $t \gg t_D$, the argument $x = Dt/r^2$ of the function $U(x)$ in Eq. (20) is large for any $\mathbf{r}_1$ and $\mathbf{r}_2$, and the functions $U_{\mathrm{FID}}(x)$ and $U_{\mathrm{SE}}(x)$ in Eq. (20) can be substituted by their asymptotic expressions (22). As expected, in this case we obtain a mono-exponential behavior of the signal

$$s_{\mathrm{FID}}(t) = \exp\left(-\Delta R_2^*\cdot t\right), \quad s_{\mathrm{SE}}(t) = \exp(-\Delta R_2\cdot t), \tag{25}$$

where ΔR_2, ΔR_2^* are given in Eq. (4).

This equation is valid for objects of arbitrary geometry, provided that the integral in Eq. (4) exists. One can draw an analogy between the integral in Eq. (4) and that appearing in the calculation of the Coulomb (electrostatic) self-energy W of a charged object with a uniform unit charge density,

$$W = \frac{1}{2}\int\int_{v_0}\frac{d\mathbf{r}_1\, d\mathbf{r}_2}{|\mathbf{r}_1 - \mathbf{r}_2|}. \tag{26}$$

Such an analogy allows calculation of the integral in Eq. (4) by means of numerous powerful methods developed in electrostatics. Note that the integral in Eq. (4) diverges if one of the object's dimensions tends to infinity. In particular, Eq. (4) cannot be applied for an infinite cylinder, for which a time dependence of the attenuation function in the long-time limit is not linear in t but contains logarithmic terms (see below).

2.2. Short-time limit

At $t \to 0$, the propagator $P(\mathbf{r}_1, \mathbf{r}_2, t)$ in Eq. (18) can be substituted by its initial value $P(\mathbf{r}_1, \mathbf{r}_2, 0) = \delta(\mathbf{r}_1 - \mathbf{r}_2)$, and the correlation function tends to $G(0)$. However, the next term in t cannot be obtained by a standard expansion of the propagator $P(\mathbf{r}_1, \mathbf{r}_2, t)$ as a series in t due to its non-analytical time dependence. As shown in Appendix B, the short-time behavior of the correlation function is

$$G(t) \simeq G(0)\cdot\left[1 - \frac{s_0}{v_0}\left(\frac{Dt}{\pi}\right)^{1/2}\right] + o(t^{1/2}), \tag{27}$$

where s_0 is the surface area of the object.

Opposite to the long-time limit, in the short-time limit the small-x asymptotic form of the function $U(x)$ cannot be used because for an arbitrary small t, there are some coordinates $\mathbf{r}_1$ and $\mathbf{r}_2$, for which the argument $x = Dt/(\mathbf{r}_1 - \mathbf{r}_2)^2$ is not small. In this case, however, we can use the short-time expansion of the correlation function $G(t)$ (27). Substituting Eq. (27) in Eq. (17), we obtain for the signal attenuation functions $\Gamma(t)$:

$$\Gamma_{\rm FID}(t) \simeq \frac{2\zeta(\delta\omega_s)^2}{45} t^2 \left[1 - \frac{8}{15}\frac{s_0}{v_0}\left(\frac{Dt}{\pi}\right)^{1/2}\right] + o(t^{5/2}), \quad (28)$$

$$\Gamma_{\rm SE}(t) \simeq \frac{8(\sqrt{2}-1)\zeta(\delta\omega_s)^2}{675} \frac{s_0}{v_0}\left(\frac{2D}{\pi}\right)^{1/2} t^{5/2} + o(t^{5/2}). \quad (29)$$

It is worth noting that the leading t^2-term in the FID signal is universal: it depends on objects' geometry only through their volume fraction ζ and is independent of their shape. The absence of the diffusion coefficient in the t^2-term shows that it originates from static dephasing processes (taking the delta-function rather than the time-dependent propagator $P(\mathbf{r}_1, \mathbf{r}_2, t)$ means neglecting diffusion).

The presence of the surface area s_0 in Eq. (29) manifests that the objects' shape and not just their volume fraction plays a crucial role in formation of the SE signal in the short-time interval. The physical origin of the $t^{5/2}$ time dependence can be explained as follows. On an object's surface the induced local magnetic field $h(\mathbf{r})$ is discontinuous and the Larmor frequency has a "jump" $\Delta\omega$ (its value varies along the object's surface). At very short times, the main contribution to the SE signal change (proportional to $(\Delta\varphi)^2$) comes from the spins crossing the objects' surface because only they experience an irreversible phase change $\Delta\varphi \sim \Delta\omega \cdot t$. To cross the surface during the time t, a spin must be located in the vicinity of the surface at the characteristic diffusion distance $(Dt)^{1/2}$. Thus, multiplying $(\Delta\varphi)^2$ (proportional to t^2) by the number of spins crossing the surface (proportional to $(Dt^{1/2}s_0/v_0)$, we obtain the dependence $\Gamma_{\rm SE} \sim (s_0/v_0)D^{1/2}t^{5/2}$ presented in Eq. (29). If there is no discontinuity in the Larmor frequency, the term proportional to $t^{5/2}$ in the SE signal attenuation at short times is expected to be absent and the usual t^3-dependence for diffusion in the presence of field gradients should be anticipated [24,25].

3. Specific geometrical models

In this section we apply the general expressions obtained above to several shapes of the magnetized objects: spheres, infinitely long cylinders, and ellipsoids of revolution.

3.1. Spheres

The model of magnetized spheres was first studied in [26], where the correlation function has been found; the relaxation rate ΔR_2 in the long-time limit in this model has been found by Jensen and Chandra [10]. We will make the next step in this direction and obtain an explicit expression for the FID and SE signals in the spherical model. For a sphere of radius R, the integral (18) can be calculated giving the correlation function $G(t)$:

$$G(t) = G_0 Q_s\left(\frac{R^2}{Dt}\right),$$
$$Q_s(x) = \frac{1}{\pi^{1/2}x^{3/2}}[(x-2)e^{-x} + 2 - 3x] + \Phi(x^{1/2}), \quad (30)$$

where $\Phi(x)$ is the error function. In such a form, the correlation function has been obtained in [10] (with different notations). The short- and long-time behaviors of the correlation function (30) is

$$G(t) \simeq G_0 \cdot \begin{cases} 1 - \frac{3}{R}\left(\frac{Dt}{\pi}\right)^{1/2}, & t \ll t_D, \\ \frac{R^3}{6\pi^{1/2}(Dt)^{3/2}}, & t \gg t_D, \end{cases} \quad (31)$$

where $t_D = R^2/D$ is the characteristic diffusion time. Eq. (31) is in agreement with the general expressions (23) and (27) (for spheres, the surface-to-volume ratio is $s_0/v_0 = 3/R$).

Making use of the correlation function (30) and Eqs. (17), an exact analytical expression for the signal attenuation function $\Gamma(t)$ can be found

$$\Gamma_{\rm FID}(t) = \frac{G_0 t_D^2}{70} \cdot \left\{35\tau^2\Phi(\tau^{-1/2}) + \frac{8}{\pi^{1/2}}\tau^{5/2}(2\tau - 7) + 4(\tau+3)\tilde{\Phi}(\tau^{-1/2}) - 2\left(\frac{\tau}{\pi}\right)^{1/2} \times e^{-1/\tau}(6 + 11\tau - 20\tau^2 + 8\tau^3)\right\}, \quad (32)$$

$$\Gamma_{\rm SE}(t) = \frac{G_0 t_D^2}{35} \cdot \left\{4(7\tau+6)\tilde{\Phi}\left((2/\tau)^{1/2}\right) - 2(7\tau+3) \times \tilde{\Phi}\left(\tau^{-1/2}\right) + \frac{2\sqrt{2}}{\pi^{1/2}}\tau^{5/2}\left[7(\sqrt{2}-1) + \tau(1-2\sqrt{2})\right] + \frac{35}{2}\tau^2\left[\Phi\left((2/\tau)^{1/2}\right) - \Phi\left(\tau^{-1/2}\right)\right] - \left(\frac{\tau}{\pi}\right)^{1/2} \times \left[\sqrt{2}e^{-2/\tau}(12 + 11\tau - 10\tau^2 + 2\tau^3) - e^{-1/\tau}(6 + 11\tau - 20\tau^2 + 8\tau^3)\right]\right\}, \quad (33)$$

where $\tau = t/t_D$. The time dependence of the signal attenuation functions $\Gamma_{\rm FID}$ and $\Gamma_{\rm SE}$ is shown in Fig. 1 (solid lines).

The short-time expansion of Eqs. (32) and (33) gives

$$\Gamma(t) \simeq \frac{2\zeta(\delta\omega_s)^2}{45} \cdot \begin{cases} t^2\left[1 - \frac{8}{5\pi^{1/2}}\left(\frac{Dt}{R^2}\right)^{1/2} + \frac{16}{35\pi^{1/2}}\left(\frac{Dt}{R^2}\right)^{3/2}\right], & \text{FID}, \\ \frac{4}{5\pi^{1/2}}\left(\frac{Dt}{R^2}\right)^{5/2}\left[(2-\sqrt{2}) - \frac{(4-\sqrt{2})}{7}\left(\frac{Dt}{R^2}\right)\right], & \text{SE}, \end{cases} \quad t \ll t_D. \quad (34)$$

Note that the next terms in the short-time expansion of $\Gamma(t)$ are non-analytical but proportional to $\exp(-t_D/t)$.

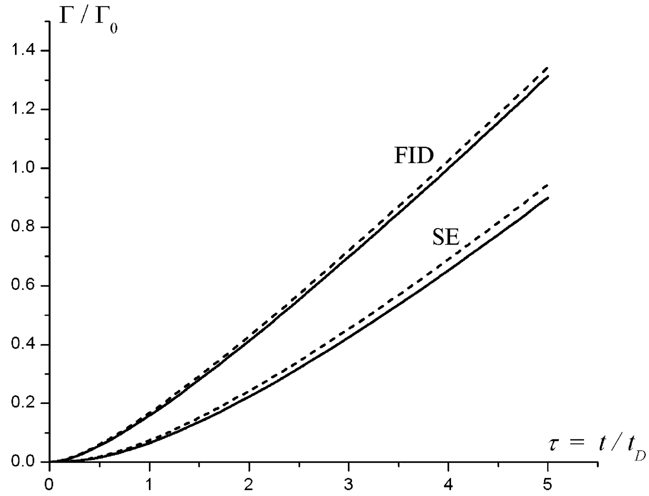

Fig. 1. The attenuation function $\Gamma(t)$ ($\Gamma \equiv -\ln(S/S_0)$, where S is the signal) for the FID and SE signals in the spherical model, normalized to $\Gamma_0 = G_0 t_D^2 = 4/45 \cdot \zeta \cdot (\delta\omega_s)^2 \cdot (R^2/D)^2$, as a function of the dimensionless time $\tau = t/t_D$. Solid lines correspond to the exact (within the Gaussian approach) expressions (32) and (33), dashed lines correspond to approximation (36).

The first two terms in $\Gamma_{\rm FID}$ and the first term in $\Gamma_{\rm SE}$ are in agreement with the general expressions (28) and (29). In the long-time limit ($t \gg t_D$), the attenuation function is linear in t with the relaxation rate

$$\Delta R_2 = \frac{8\zeta(\delta\omega_s)^2 R^2}{225D}. \tag{35}$$

The same result can be easily obtained from electrostatic analogy (26). Indeed, in the case of spherical objects with radius R, the Coulomb energy is $W = 16\pi^2 R^5/15$, which immediately leads to Eq. (35).

This result for ΔR_2 coincides with that obtained in [10] (different notations are used) by means of calculation of the correlation function on the basis of an explicit expression for a magnetic field induced by spheres. As shown in [27] and reiterated in [28], ΔR_2 given in Eq. (35) differs by a numerical factor 10/9 from that obtained in the framework of the outer sphere model. This is because in the latter model the spheres are supposed to be impenetrable for diffusing spins, whereas in [10] and in the model presented here unrestricted diffusion is assumed.

Note that the rather cumbersome results in Eqs. (32) and (33) for the signal attenuation functions can be approximated by relatively simple expressions:

$$\begin{aligned}\Gamma_{\rm FID}(t) &\simeq \frac{2G_0 t_D^2}{25}\left[(1+5\tau)^{1/2}-1\right]^2,\\ \Gamma_{\rm SE}(t) &\simeq \frac{2G_0 t_D^2}{25}\left\{4\left[(1+5\tau/2)^{1/2}-1\right]^2 - \left[(1+5\tau)^{1/2}-1\right]^2\right\}.\end{aligned} \tag{36}$$

The approximations (36) are shown in Fig. 1 by dashed lines.

3.2. Infinitely long cylinders

For a infinitely long cylinder of radius R with the axis oriented along the Cartesian axis z, the integration limits in Eq. (18) are given by the inequality $x^2 + y^2 \leqslant R^2$, leading to the correlation function

$$\begin{aligned}G(t) &= G_0 Q_c\left(\frac{R^2}{Dt}\right),\\ Q_c(x) &= 1 - e^{-x/2}\left[I_0\left(\frac{x}{2}\right) + I_1\left(\frac{x}{2}\right)\right],\end{aligned} \tag{37}$$

where $I_0(x)$ and $I_1(x)$ are the modified Bessel functions of zero and first order.

The short- and long-time behaviors of the correlation function (37) is

$$G(t) \simeq G_0 \cdot \begin{cases} 1 - \frac{2}{R}\left(\frac{Dt}{\pi}\right)^{1/2}, & t \ll t_D,\\ \frac{R^2}{4Dt}, & t \gg t_D. \end{cases} \tag{38}$$

In the short-time limit, Eq. (38) is in agreement with the general expressions (27) (for cylinder, the surface-to-volume ratio is $s_0/v_0 = 2/R$), whereas in the long-time limit the correlation function coincides with Eq. (24).

Making use of the correlation function (37) and Eqs. (17), an exact analytical expressions for the signal attenuation function $\Gamma(t)$ can be found:

$$\Gamma_{\rm FID}(t) = G_0 t_D^2 \cdot \left[\frac{5}{768\tau}\,{}_3F_3\left(\left\{1,1,\frac{7}{2}\right\},\{3,4,5\},-\frac{1}{\tau}\right) + \frac{\tau\ln\tau}{4} + C_1\tau + \frac{\ln\tau}{16} + C_2\right], \tag{39}$$

$$\Gamma_{\rm SE}(t) = G_0 t_D^2 \cdot \left\{\frac{5}{768\tau}\left[8\cdot{}_3F_3\left(\left\{1,1,\frac{7}{2}\right\},\{3,4,5\},-\frac{2}{\tau}\right) - {}_3F_3\left(\left\{1,1,\frac{7}{2}\right\},\{3,4,5\},-\frac{1}{\tau}\right)\right] + \frac{\tau\ln\tau}{4} + C_3\tau + \frac{3\ln\tau}{16} + C_4\right\}. \tag{40}$$

Here ${}_3F_3(\cdots)$ is the generalized hypergeometric function [23], the numerical constant $C_1 = (4\ln 2 - 1 - 2C)/8 \approx 0.077$, $C_2 = (5 + 6\ln 2 - 3C)/48 \approx 0.155$, $C_3 = -(1+2C)/8 \approx -0.269$, $C_4 = (5 + 2\ln 2 - 3C)/16 \approx 0.291$, and $C \approx 0.577$ is the Euler constant. The time dependence of the functions $\Gamma_{\rm FID}$ (39) and $\Gamma_{\rm SE}$ (40) are shown in Figs. 2a and b (solid lines).

In the short-time limit, $t \ll t_D$, the signal attenuation function $\Gamma(t)$ reduces to

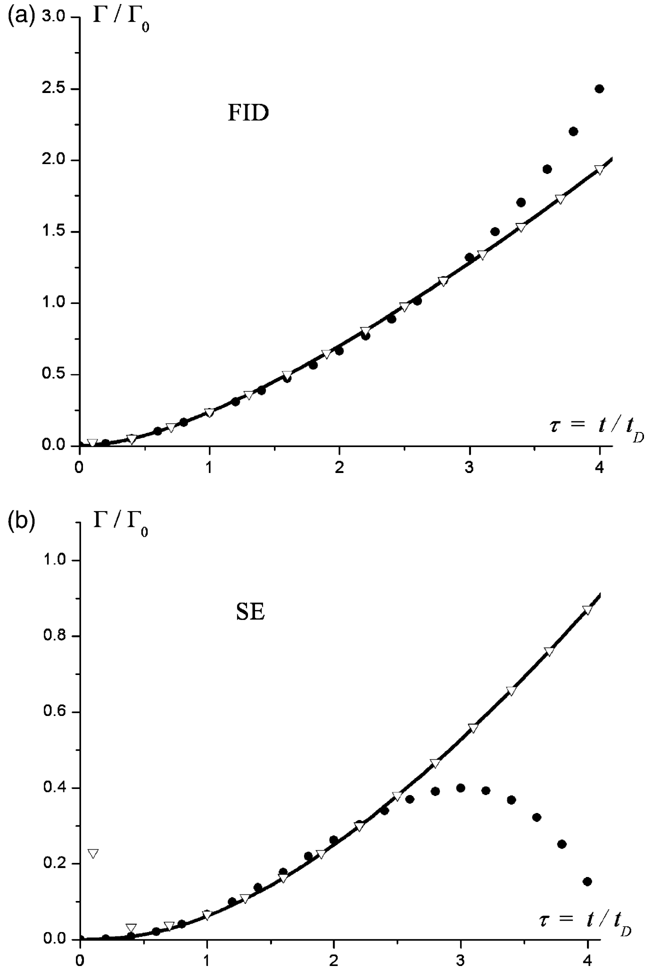

Fig. 2. The attenuation function $\Gamma(t)$ for the FID signal (a) and SE signal (b) in the cylindrical model, normalized to $\Gamma_0 = G_0 t_D^2 = 4/45 \cdot \zeta \cdot (\delta\omega_s)^2 \cdot (R^2/D)^2$, as a function of the dimensionless time $\tau = t/t_D$. Solid lines correspond to the exact formulas (39) and (40); circles correspond to the short-time approximation (41); triangles correspond to the long-time approximation (42).

$$\Gamma(t) \simeq \frac{2\zeta(\delta\omega_s)^2}{45} \cdot \begin{cases} t^2\left[1 - \frac{16}{5\pi^{1/2}}\left(\frac{Dt}{R^2}\right)^{1/2} + \frac{4}{35\pi^{1/2}}\left(\frac{Dt}{R^2}\right)^{3/2}\right], & \text{FID}, \\ \frac{1}{5\pi^{1/2}}\left(\frac{Dt}{R^2}\right)^{5/2}\left[\frac{8(2-\sqrt{2})}{3} - \frac{(4-\sqrt{2})}{7}\left(\frac{Dt}{R^2}\right)\right], & \text{SE}, \end{cases} \quad t \ll t_D. \tag{41}$$

The first two terms in $\Gamma_{\rm FID}$ and the first term in $\Gamma_{\rm SE}$ are in agreement with the general expressions (28) and (29).

It can be shown that for $\tau > 1$ the hypergeometric functions in Eqs. (39) and (40) are approximately equal to 1 and the attenuation functions $\Gamma(t)$ are well described by simple expressions

$$\Gamma_{\rm FID}(t) \simeq G_0 t_D^2 \cdot \left(\frac{\tau \ln \tau}{4} + C_1\tau + \frac{\ln\tau}{16} + C_2 + \frac{5}{768\tau}\right),$$
$$\Gamma_{\rm SE}(t) \simeq G_0 t_D^2 \cdot \left(\frac{\tau \ln \tau}{4} + C_3\tau + \frac{3\ln\tau}{16} + C_4 + \frac{35}{768\tau}\right). \tag{42}$$

Aside from notation differences, the first four terms in Eq. (42) coincides with the asymptotic behavior of $\Gamma(t)$ in the motional narrowing regime $(t \gg t_D)$ obtained for the cylindrical model by Kiselev and Posse [7]. However, in the interval $\tau < 3$ the last term gives a substantial contribution to Γ.

The long-time approximations (42) (triangles) as well the short-time expressions (41) (circles) are shown in Figs. 2a and b. Although the short-time approximations (41) are obtained in the limiting case $t \ll t_D$, in fact, Eq. (41) is valid in a rather broad range: the function $\Gamma(t)$ can be accurately described by the short-time expressions in the interval at $t < 3.4t_D$ for the FID signal and $t < 2.7t_D$ for the SE signal with an error not exceeding 10% at the upper end of the intervals. The long-time expressions (42) are also valid not only for $t \gg t_D$: Eq. (42) approximate the signal in the intervals $t > 0.3t_D$ for the FID signal and $t > 0.9t_D$ for the SE signal with an error not exceeding 10% at the lower end of the intervals.

3.3. Ellipsoids of revolution

An ellipsoid of revolution can be obtained by rotating an ellipse about one of its axes. For an ellipse with the half-axes a and b and with the symmetry axis (let it be b) parallel to the Cartesian axis z, the integration limits in Eq. (18) are given by the inequality

$$\frac{x^2+y^2}{a^2} + \frac{z^2}{b^2} \leqslant 1. \tag{43}$$

Evaluating the integral in Eq. (18) in these limits, the correlation function $G(t)$ in case of spheroidal objects can be written in the form:

$$G(t) = \frac{6G_0}{\pi} \cdot \int_0^\infty u\,{\rm d}u \int_0^\infty {\rm d}v \exp\left(-\frac{tu^2}{t_a} - \frac{tv^2}{t_b}\right) \cdot \frac{(\sin\tilde{q} - \tilde{q}\cos\tilde{q})^2}{\tilde{q}^6}, \quad \tilde{q} = (u^2+v^2)^{1/2}, \tag{44}$$

where $t_a = a^2/D$ and $t_b = b^2/D$ are the characteristic diffusion times. In the limiting case of spheres, $a = b$, the integral in Eq. (44) can be evaluated analytically and the correlation function reduces to Eq. (30).

In the short-time limit, when t is much smaller than both the characteristic diffusion times, $t \ll t_a$, $t \ll t_b$, the correlation function and FID and SE signals are described by the general expression (27)–(29) with the surface-to-volume ratio

$$\begin{aligned} \frac{s_0}{v_0} &= \frac{3}{2b}\left(1 + \frac{b}{a\varepsilon}\arcsin\varepsilon\right), \\ \varepsilon &= \left(1 - \frac{a^2}{b^2}\right)^{1/2}, \quad a < b \text{ (prolate spheroid)}, \\ \frac{s_0}{v_0} &= \frac{3}{2b}\left(1 + \frac{b^2}{2a^2\varepsilon_1}\ln\frac{1+\varepsilon_1}{1-\varepsilon_1}\right), \\ \varepsilon_1 &= \left(1 - \frac{b^2}{a^2}\right)^{1/2}, \quad a > b \text{ (oblate spheroid)}. \end{aligned} \tag{45}$$

In the long-time limit, when t is much longer than the characteristic times, $t \gg t_a$, $t \gg t_b$, only small values of u and v contribute to the integral (44), and the correlation function takes the form

$$G(t) \simeq \frac{G_0}{6\pi^{1/2}} \frac{a^2 b}{(Dt)^{3/2}} \sim t^{-3/2}. \tag{46}$$

If the half-axes of the spheroid are substantially different, for example, $b \gg a$ (long "cigar" geometry), there is an intermediate time regime $t_a \ll t \ll t_b$ where the correlation function can be approximated by an expression similar to that for the model of cylinders

$$G(t) \simeq \frac{G_0}{5} \frac{a^2}{Dt} \sim t^{-1}. \tag{47}$$

As for cylinders, in this time interval diffusion can be effectively considered as two-dimensional because diffusion along the long spheroid axis does not affect the correlation function (the magnetic field induced by a "cigar" is practically uniform along its long axis). In the opposite case, $b \ll a$ (thin "pancake" geometry), there is an intermediate time regime when $t_b \ll t \ll t_a$ where the correlation function can be approximated by

$$G(t) \simeq \frac{3G_0}{4\pi^{1/2}} \frac{b}{(Dt)^{1/2}} \sim t^{-1/2}. \tag{48}$$

It is easy to see that such a correlation function effectively corresponds to one-dimensional diffusion along the normal to the "pancake."

Using Eq. (44), the FID and SE signal attenuation functions for the spheroidal model can be written in the form

$$\Gamma(t) = \frac{24\zeta(\delta\omega_s)^2}{45\pi} \cdot \int_0^\infty u\,\mathrm{d}u \int_0^\infty \mathrm{d}v \cdot \frac{\left(\sin\tilde{q} - \tilde{q}\cos\tilde{q}\right)^2}{\tilde{q}^6} \cdot g\left(\frac{u^2}{t_a} + \frac{v^2}{t_b}, t\right) \tag{49}$$

where $g(x,t)$ is given by Eq. (A.19).

In the short-time limit, the attenuation function is described by the general expressions (28) and (29). To calculate the relaxation rate ΔR_2 (or ΔR_2^*) in the long-time limit $t \gg t_a, t_b$, it is more convenient to use not the general expression (4) but Eq. (49). In this limit, $g(x,t) \simeq t/x$ for both the FID and SE signals, and $\Gamma(t) \simeq R_2 \cdot t$, where

$$\Delta R_2 = \frac{8\zeta(\delta\omega_s)^2}{225} \cdot \frac{\overline{R}^2}{D} \cdot L(\kappa), \qquad L(\kappa) = \kappa^{2/3} \cdot \frac{\arctan(\kappa^2 - 1)^{1/2}}{(\kappa^2 - 1)^{1/2}}, \tag{50}$$

where $\kappa = a/b$ and $\overline{R} = (3v_0/4\pi)^{1/3}$. Eq. (50) demonstrates the dependence of the relaxation rate ΔR_2 on the object's shape (when a volume of the object is fixed), in this particular case, on the aspect ratio $\kappa = a/b$. This dependence is described by the function $L(\kappa)$, which is plotted in Fig. 3.

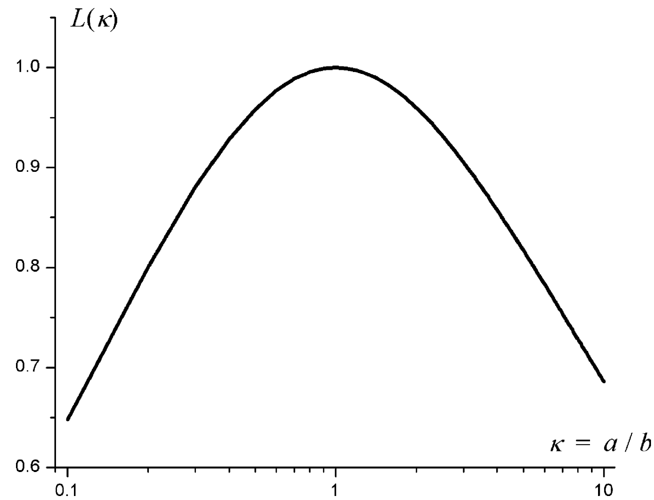

Fig. 3. The function $L(\kappa)$ (50) describing the dependence of the relaxation rate constant ΔR_2 in the ellipsoidal model on the aspect ratio $\kappa = a/b$ for a fixed particle volume v_0 The maximum at $\kappa = 1$ corresponds to spheres.

The function $L(\kappa)$ has a maximum $L = 1$ at $\kappa = 1$ (sphere, see Eq. (35)) and tends to 0 at $\kappa \to 0$ and $\kappa \to \infty$

$$L(\kappa) \simeq \begin{cases} \kappa^{2/3} \ln\frac{2}{\kappa}, & \kappa \ll 1, \\ \frac{\pi}{2\kappa^{1/3}}, & \kappa \gg 1. \end{cases} \tag{51}$$

For the latter limits (formally, corresponding to an infinitely long cylinder and an infinite plane, respectively) the long-time behavior of the signal, as mentioned above, is not mono-exponential and cannot be described by the relaxation rate ΔR_2 (the "Coulomb" integral in Eq. (4) diverges).

4. Discussion

In the short-time limit, the FID signal is shown to have the universal t^2 time dependence (characteristic of the static dephasing regime) and depends on the objects' geometry only through their volume fraction ζ. This result is based on a surprising property of the system containing uniformly distributed and uniformly oriented magnetized objects: the correlation function $G(0) \equiv \langle\omega^2\rangle$ depends only on the objects' susceptibility and their volume fraction ζ. The physical origin of such independence on the objects' shape is rather simple: although the symmetry of the magnetic field induced by each particular object is determined by its specific geometry, positional and orientational averaging "restore" the spherical symmetry of the system as a whole (no preferred directions). The t^2-behavior at short times is a general feature of the FID signal in the static dephasing regime [29]. For particular cases of spherical, cylindrical, and ellipsoidal objects, this behavior has been obtained previously in [6,14,22]. It should be mentioned that in [22], where the FID signal has been analyzed for ellipsoids of revolution (spheroids) as the magnetized objects, the signal from the inner volume of the objects (the internal dephasing function s_i) and from outside space (the external dephasing function s_e) are given separately[1] and described in the short-time limit by Eq. (38) and Eqs. (39)–(41) in Ref. [22], respectively. If we, however, combine these two contributions to the total signal and take into account the inequality $\zeta \ll 1$, we obtain the t^2-time dependence of the FID signal with the coefficient independent from a spheroid's half-axes ratio in complete agreement with the leading term in Eq. (28).

If the number of the objects is small or their positions and/or orientations are not uniform, the global symmetry of the system is not spherical and $G(0)$ cannot be described, in general, by a geometry-independent expression. Obviously, Eq. (4) is valid only for a small volume fraction ζ. If $\zeta \to 1$, we can consider the objects as a new "media" and the media as new "objects" with the volume fraction $(1-\zeta)$. In this case, the quantity $G(0)$ will be proportional to $(1-\zeta)$. As proposed in [12], the case of an arbitrary volume fraction can be described by a simple polynomial interpolation $\zeta \to \zeta \cdot (1-\zeta)$. Such a modification should be done in Eq. (4) and all other formulas containing the volume fraction ζ.

The SE signal decay in the short-time limit is mainly caused by spins diffusing across the objects' surface. The corresponding attenuation function is proportional to $(D^{1/2}\, t^{5/2})$ with a coefficient depending on the objects' surface-to-volume ratio. Note that the surface-to-volume ratio also appears in another problem, where the role of spins located in the vicinity of boundaries is also crucial, namely, in the theory of apparent diffusion coefficient in porous media [30]. In this theory, however, spins are reflected from surfaces (or partially absorbed by them) and diffusion is analyzed in the presence of a constant field gradient.

In the motional narrowing regime the FID and SE signals decay mono-exponentially with the relaxation rate constants ΔR_2^* and ΔR_2, respectively, Eq. (4), provided that the "Coulomb" integral in Eq. (4) exists. For infinite cylinders, in the motional narrowing regime the signal decays non-exponentially (see Eq. (42)).

If the magnetized objects can be characterized by a single characteristic size R, the expression for the signal can be represented in the form

$$S(t) = S_0 \exp[-\Gamma(t)],$$
$$\Gamma(t) = \eta \cdot \zeta \cdot (\delta\omega_s)^2 \cdot t_D^2 \cdot F\left(\frac{t}{t_D}\right), \tag{52}$$

where $t_D = R^2/D$, the numerical coefficient η and the function $F(\tau)$ depend on the shape of the objects (see, e.g. Eqs. (32) and (33) and (39) and (40)). If we are interested in the R-dependence of the signal attenuation function for a fixed acquisition time t, it is convenient to re-write Eq. (52) in the form

$$\Gamma = \eta \cdot \zeta \cdot (\delta\omega_s \cdot t)^2 \cdot \overline{F}(\tau), \quad \tau = t/t_D = Dt/R^2, \tag{53}$$

where $\overline{F}(\tau) = F(\tau)/\tau^2$. Using the general properties of the function $F(\tau)$, it can be readily shown that for small characteristic sizes, $R \ll (Dt)^{1/2}$, the function $\overline{F}$ tends to zero as $\overline{F} \sim R^2$ (or $\overline{F} \sim R^2|\ln R|$ for infinitely long cylinders). For large characteristic sizes, $R \gg (Dt)^{1/2}$, the function $\overline{F}$ becomes R-independent for the FID signal and tends to zero as $\overline{F} \sim 1/R$ for the SE signal. Hence, for the SE signal the attenuation function Γ as a function of R has a maximum at some characteristic size $R = R_m = (Dt/\tau_m)^{1/2}$, where τ_m is determined by the equation $\overline{F}'(\tau_m) = 0$. The value of this attenuation function at this maximum is proportional to the volume fraction and to the echo time squared, and inversely proportional to the external field, $\Gamma_{\max} \sim \zeta \cdot t^2/H_0^2 \cdot \overline{F}_{\max}$, where $\overline{F}_{\max} = \overline{F}(\tau_m)$ (as well as τ_m) is determined only by the objects' shape. As the echo time t increases, $\Gamma_{\max}$ also increases as t^2 and its position on the R-axis shifts to higher values: $R_m \sim t^{1/2}$. These results are consistent with the numerical calculations by Boxerman et al. (see Fig. 7 in [5]).

Acknowledgments

The authors are grateful to Professors Mark S. Conradi and Joseph J.H. Ackerman for substantial and helpful comments. This work is supported in part by NIH Grant R01 NS4519-01A1.

Appendix A. Correlation function *G*(*t*)

Consider a system consisting of a large number N, $N \gg 1$, of magnetized objects of magnetic susceptibility χ_i embedded in a medium with another susceptibility χ_e. In the presence of an external homogeneous magnetic field $\mathbf{H}_0$, these objects create an additional inhomogeneous mesoscopic magnetic field $\delta\mathbf{H}(\mathbf{r})$:

$$\delta\mathbf{H}(\mathbf{r}) = \sum_{n=1}^{N} \mathbf{h}_n(\mathbf{r} - \mathbf{R}_n). \tag{A.1}$$

Here $\mathbf{h}_n$ is a contribution of the nth object located at the point $\mathbf{R}_n$. The local NMR frequency at the position $\mathbf{r}$,

[1] In Ref. [22]. A.L. Sukstanskii and D.A. Yablonskiy, Theory of FID NMR signal dephasing induced by mesoscopic magnetic field inhomogeneities in biological systems, J. Magn. Reson. 151 (2001) 107 there is a misprint in Eq. (37) for the internal dephasing function s_i: an erroneous factor $\exp(ip)$ should be substituted by $\exp(ip/3)$. The asymptotic expressions (38) are correct.

$\omega(\mathbf{r})$, has contributions from all objects and is equal to $\omega(\mathbf{r}) = \gamma H(\mathbf{r})$, where γ is the gyromagnetic ratio, $H(\mathbf{r})$ is the projection of the local nuclear magnetic field $\mathbf{H}(\mathbf{r})$ onto the direction of the external field $\mathbf{H}_0$. In the Lorentzian approximation (see, e.g. [31]), which is fairly precise for isotropic liquids, $\mathbf{H}(\mathbf{r}) = \mathbf{H}_0(1 + 4\pi\chi_e/3) + \delta\mathbf{H}(\mathbf{r})$ in the medium and $\mathbf{H}(\mathbf{r}) = \mathbf{H}_0(1 + 4\pi\chi_i/3) + \delta\mathbf{H}(\mathbf{r})$ inside the objects (we assume that the magnetic susceptibilities $\chi_{i,e}$ are small enough to ignore effects nonlinear in χ). In what follows, the frequency $\omega_0 = \gamma H_0(1 + 4\pi\chi_e/3)$ will be considered as the frequency of the rotating frame, and all results will be presented with respect to this reference frequency. In fact, the system under consideration can be treated as a system consisting of the magnetized objects with a relative susceptibility $\Delta\chi = \chi_i - \chi_e$ embedded in a non-magnetic medium with $\chi = 0$. The Lorentz field in this approach differs from zero only within the objects and is equal to $4\pi\Delta\chi\mathbf{H}_0/3$.

The correlation function $G(t)$ (16) can be written in the form

$$G(t) = \frac{\gamma^2}{V}\left\langle \int\int \mathrm{d}\mathbf{r}_1\, \mathrm{d}\mathbf{r}_2 P(\mathbf{r}_1, \mathbf{r}_2, t) \cdot \widetilde{G}(\mathbf{r}_1, \mathbf{r}_2) \right\rangle_{\text{orientation}}, \tag{A.2}$$

where

$$\begin{aligned}\widetilde{G}(\mathbf{r}_1, \mathbf{r}_2) &= \left\langle \sum_{n,m} h(\mathbf{r}_1 - \mathbf{R}_n) h(\mathbf{r}_2 - \mathbf{R}_m) \right\rangle_{\text{position}} \\ &= \left\langle \sum_{n}^{N} h(\mathbf{r}_1 - \mathbf{R}_n) h(\mathbf{r}_2 - \mathbf{R}_n) \right\rangle_{\text{position}} \\ &\quad + \left\langle \sum_{n \neq m} h(\mathbf{r}_1 - \mathbf{R}_n) h(\mathbf{r}_2 - \mathbf{R}_m) \right\rangle_{\text{position}},\end{aligned} \tag{A.3}$$

where $h(\mathbf{r} - \mathbf{R}_n)$ is the projection of the local nuclear magnetic field created by the nth object located at the point $\mathbf{R}_n$ on the direction of the external field $\mathbf{H}_0$. Since the object positions $\mathbf{R}_n$ are uniformly distributed over the system volume V, position averaging of any function of $\mathbf{R}_n$ means

$$\langle f(\mathbf{R}_n) \rangle_{\text{position}} = \frac{1}{V} \int \mathrm{d}\mathbf{R}_n f(\mathbf{R}_n). \tag{A.4}$$

Note that Eq. (A.4) allows overlapping of the magnetized objects, so for real particles (which can not overlap) this is right only in dilute limit (small volume fraction).

Averaging the non-diagonal terms in Eq. (A.3) gives zero. Substituting the diagonal term of Eq. (A.3) in Eq. (A.2) and using the fact that the propagator $P(\mathbf{r}_1, \mathbf{r}_2, t)$ is a function of the difference $(\mathbf{r}_1 - \mathbf{r}_2)$, the correlation function $G(t)$ takes the form

$$G(t) = \frac{\gamma^2 N}{V}\left\langle \int\int \mathrm{d}\mathbf{r}_1\, \mathrm{d}\mathbf{r}_2 P(\mathbf{r}_1, \mathbf{r}_2, t) \cdot h(\mathbf{r}_1) h(\mathbf{r}_2) \right\rangle_{\text{orientation}}, \tag{A.5}$$

where $h(\mathbf{r})$ is the field induced by one object located at the coordinate origin.

Using the Fourier representation of the propagator $P(\mathbf{r}_1, \mathbf{r}_2, t)$,

$$\begin{aligned}\tilde{P}(\mathbf{k}, t) &= \int \mathrm{d}\mathbf{r} \exp(-\mathrm{i}\,\mathbf{k}(\mathbf{r}_1 - \mathbf{r}_2)) P(\mathbf{r}_1, \mathbf{r}_2, t) \\ &= \exp(-D\mathbf{k}^2 t).\end{aligned} \tag{A.6}$$

Eq. (A.5) can be re-written in the form

$$G(t) = \frac{\gamma^2 N}{V} \cdot \left\langle \int \frac{\mathrm{d}\mathbf{k}}{(2\pi)^3} \exp(-D\mathbf{k}^2 t) \left|\tilde{h}(\mathbf{k})\right|^2 \right\rangle_{\text{orientation}}, \tag{A.7}$$

where $\tilde{h}(\mathbf{k})$ is the Fourier transformation of $h(\mathbf{r})$.

The field $\mathbf{h}(\mathbf{r})$ induced by one object with the relative susceptibility $\Delta\chi = \chi_i - \chi_e$ embedded in the non-magnetic medium can be found by solving the Laplace equation for the magnetic potential Φ,

$$\mathbf{h} = -\nabla\Phi, \quad \nabla^2\Phi = 4\pi\,\mathrm{div}\mathbf{M}, \tag{A.8}$$

where $\mathbf{M}$ is the magnetization vector induced by the external field $\mathbf{H}_0$ within the object. The magnetization $\mathbf{M}$ relates to the total magnetic field $\mathbf{H}$ within the object as $\mathbf{M} = \Delta\chi \cdot \mathbf{H}$. Neglecting nonlinear in χ terms, the field $\mathbf{H}$ can be substituted by the external field $\mathbf{H}_0$, $\mathbf{M} \simeq \Delta\chi \cdot \mathbf{H}_0$. It is important to note that in this approximation the magnetization $\mathbf{M}$ is uniform within the objects and $\mathbf{M} = 0$ outside.

Solving Eq. (A.8) in the Fourier domain, we get

$$\begin{aligned}\tilde{\mathbf{h}}(\mathbf{k}) &= -\frac{4\pi\mathbf{k}(\mathbf{k}\mathbf{M})}{k^2} \cdot F(\mathbf{k}) \\ &= -\frac{4\pi\Delta\chi\mathbf{k}(\mathbf{k}\mathbf{H}_0)}{k^2} \cdot F(\mathbf{k}),\end{aligned} \tag{A.9}$$

where $\tilde{\mathbf{h}}(\mathbf{k})$ is the Fourier transform of $\mathbf{h}(\mathbf{r})$ and $F(\mathbf{k})$ is the form-factor of the object,

$$F(\mathbf{k}) = \int_{v_0} \mathrm{d}\mathbf{r} \exp(-\mathrm{i}\,\mathbf{k}\mathbf{r}). \tag{A.10}$$

The integral in Eq. (A.10) is over the volume of the object. This integral can be readily evaluated for some symmetric object's geometries.

Sphere of radius R

$$F(\mathbf{k}) = \int_{x^2+y^2+z^2 \leqslant R^2} \mathrm{d}\mathbf{r} \exp(-\mathrm{i}\mathbf{k}\mathbf{r}) = \frac{4\pi}{k^3}(\sin kR - kR\cos kR). \tag{A.11}$$

Cylinder of radius R and height H (with symmetry axis oriented along the Cartesian axis z)

$$F(\mathbf{k}) = \int_{\substack{x^2+y^2\leqslant R^2\\ |z|\leqslant H/2}} \mathrm{d}\mathbf{r}\exp(-\mathrm{i}\,\mathbf{kr}) = \frac{4\pi R}{k_\perp k_z}\cdot J_1(k_\perp R)\cdot\sin\left(\frac{k_z H}{2}\right), \tag{A.12}$$

where $k_\perp = |\mathbf{k}_\perp|$, $\mathbf{k}_\perp$ is the two-dimensional vector in the basal plane of the cylinder (XY) and J_1 is the Bessel function.

Ellipsoid with half-axes a, b, and c oriented along the Cartesian axes x, y, z, respectively:

$$F(\mathbf{k}) = \int_{\frac{x^2}{a^2}+\frac{y^2}{b^2}+\frac{z^2}{c^2}\leqslant 1} \mathrm{d}\mathbf{r}\exp(-\mathrm{i}\,\mathbf{kr}) = \frac{4\pi abc}{q^3}(\sin q - q\cos q),$$
$$q = [(ak_x)^2 + (bk_y)^2 + (ck_z)^2]^{1/2}. \tag{A.13}$$

To obtain the local nuclear magnetic field, we should add the Lorentz field $4\pi\Delta\chi\mathbf{H}_0/3$. As this field is non-zero only inside the object (where it is uniform), its Fourier-transform is $(4\pi\Delta\chi\mathbf{H}_0/3)\cdot F(\mathbf{k})$. Hence, $\tilde{h}(\mathbf{k})$ takes the form

$$\tilde{h}(\mathbf{k}) = 4\pi\Delta\chi H_0\left(\frac{1}{3} - \cos^2\alpha_{\mathbf{k}}\right)F(\mathbf{k}), \tag{A.14}$$

where α_k is the angle between the vector $\mathbf{k}$ and the external field $\mathbf{H}_0$.

Substituting Eq. (A.14) in Eq. (A.7), the correlation function $G(t)$ takes the form

$$G(t) = \frac{\zeta(\delta\omega_s)^2}{v_0}\cdot\left\langle\int\frac{d\mathbf{k}}{(2\pi)^3}\exp(-D\mathbf{k}^2 t)\times\left(\frac{1}{3}-\cos^2\alpha_{\mathbf{k}}\right)^2|F(\mathbf{k})|^2\right\rangle_{\text{orientation}}, \tag{A.15}$$

where $\delta\omega_s = 4\pi\cdot\Delta\chi\cdot\gamma H_0$ is the characteristic frequency shift, $\zeta = Nv_0/V$ is the volume fraction occupied by the objects, v_0 is the volume of one object.

The final step is orientation averaging. For a uniform distribution of the objects' orientations, the angular distribution function is the solid-angle weighting factor, $(\sin\alpha_k)/2$, $0\leqslant\alpha_{\mathbf{k}}\leqslant\pi$. Integrating Eq. (A.15) with such a distribution function, we obtain the correlation function

$$G(t) = \frac{G_0}{v_0}\cdot\int\frac{\mathrm{d}\mathbf{k}}{(2\pi)^3}\exp(-D\mathbf{k}^2 t)|F(\mathbf{k})|^2, \tag{A.16}$$

where

$$G_0 = G(0) = \frac{4\zeta(\delta\omega_s)^2}{45}. \tag{A.17}$$

Substituting Eq. (A.16) in Eqs. (17), we obtain the function $\Gamma(t)$ in the form

$$\Gamma(t) = \frac{G_0}{v_0}\cdot\int\frac{\mathrm{d}\mathbf{k}}{(2\pi)^3}g(D\mathbf{k}^2, t)|F(\mathbf{k})|^2, \tag{A.18}$$

where the function $g(x,t)$ depends on the specific structure of the RF pulse sequence: for FID and SE signals these functions are

$$g_{\mathrm{FID}}(x,t) = \frac{1}{x^2}(\mathrm{e}^{-xt} + xt - 1),$$
$$g_{\mathrm{SE}}(x,t) = \frac{1}{x^2}\left(4\mathrm{e}^{-xt/2} - \mathrm{e}^{-xt} + xt - 3\right). \tag{A.19}$$

The expressions similar to Eqs. (A.18) and (A.19) have been obtained by solving the Bloch–Torrey equation in second order perturbation theory with respect to the small parameter $\delta\omega_s\cdot t_D$, for the particular case of infinitely long cylinders in [7] and for objects of arbitrary geometry in [12].

Coming back from the Fourier domain to the coordinate domain, the correlation function takes a rather simple and elegant form:

$$G(t) = \frac{G_0}{v_0}\cdot\int\int_{v_0}\mathrm{d}\mathbf{r}_1\,\mathrm{d}\mathbf{r}_2 P(\mathbf{r}_1,\mathbf{r}_2,t) = \frac{G_0}{v_0(4\pi Dt)^{3/2}}\cdot\int\int_{v_0}\mathrm{d}\mathbf{r}_1\,\mathrm{d}\mathbf{r}_2\exp\left[-\frac{(\mathbf{r}_1-\mathbf{r}_2)^2}{4Dt}\right], \tag{A.20}$$

where the integration is over a single object volume only. Eqs. (A.16) and (A.20) are two alternative forms for calculating $G(t)$. The first one is most convenient when the form-factor $F(\mathbf{k})$ is available in a more or less simple form (sphere, cylinder, ellipsoid, see Eqs. (A.11)–(A.13)), whereas for less symmetric objects a direct calculation of the integral in Eq. (A.20) is preferable: for any arbitrary geometry this integral can be easily evaluated numerically. In addition, the $\mathbf{r}$-domain expressions are convenient for analyzing the asymptotic behaviors of the correlation function and the signal in the short- and long-time limits.

Appendix B. The correlation function $G(t)$ in the short-time limit

As $t\to 0$, the propagator $P(\mathbf{r}_1,\mathbf{r}_2,t)$ tends to its initial value $P(\mathbf{r}_1,\mathbf{r}_2,0) = \delta(\mathbf{r}_1-\mathbf{r}_2)$ and $G(t)\to G_0$. To obtain the next term in t in the short-time limit, when $t \ll R^2/D$, we introduce a new variable $\mathbf{r} = \mathbf{r}_1 - \mathbf{r}_2$ and write down the integral in Eq. (18) in the form

$$G(t) = \frac{G_0}{v_0(4\pi Dt)^{3/2}}\cdot\int_{v_0}\mathrm{d}\mathbf{r}_1\int_{\tilde{v}_0(\mathbf{r}_1)}\mathrm{d}\mathbf{r}\exp\left[-\frac{\mathbf{r}^2}{4Dt}\right], \tag{B.1}$$

where the inner integration is over the region $\tilde{v}_0(\mathbf{r}_1)$ depending on the point $\mathbf{r}_1$. At $t\ll R^2/D$ only those $\mathbf{r}$ contribute to the inner integral for which $|\mathbf{r}|\leqslant(Dt)^{1/2}\ll R$. For each point $\mathbf{r}_1$ we can determine the point nearest to $\mathbf{r}_1$ on the object's surface (call it $\mathbf{r}_1'$) and introduce a local coordinate system (x,y,z) with the origin at $\mathbf{r}_1$ and the z-axis along the outward normal to the surface at the point $\mathbf{r}_1'$ (we suppose that the object's surface is smooth enough that a tangential plane exists for each surface points except for a countable set of them). The inner integration over $\mathbf{r}$ in (B.1) can be made in this local coordinate system, the region of integration being restricted by the object's surface. However, due to the inequality $t \ll R^2/D$ and the exponentially decreasing integrand with $|\mathbf{r}|$, only the restrictions toward the point $\mathbf{r}_1'$ can be important: $z \leqslant h$, where $h = |\mathbf{r}_1 - \mathbf{r}_1'|$. All other integration limits can be expanded to infinity, producing only exponentially small error of order $\exp(-R^2/Dt)$. Hence, the correlation function can be written as

$$G(t) \simeq \frac{G_0}{v_0 (4\pi Dt)^{3/2}} \cdot \int_{v_0} \mathrm{d}\mathbf{r}_1 \left[\int_{-\infty}^{\infty} \int_{-\infty}^{\infty} \mathrm{d}x\, \mathrm{d}y \int_{-\infty}^{h} \mathrm{d}z \exp\left(-\frac{\mathbf{r}^2}{4Dt} \right) \right] = \frac{G_0}{v_0} \cdot \int_{v_0} \mathrm{d}\mathbf{r}_1 \left[1 - \frac{1}{2} \tilde{\Phi}\left(\frac{h}{2(Dt)^{1/2}} \right) \right] = G_0 \cdot \left[1 - \frac{1}{2v_0} \int_{v_0} \mathrm{d}\mathbf{r}_1 \tilde{\Phi}\left(\frac{h}{2(Dt)^{1/2}} \right) \right], \tag{B.2}$$

where $\tilde{\Phi}(x)$ is the complementary error function, which exponentially tends to 0 for $x \geq 1$. Therefore, only points $\mathbf{r}_1$ located in the vicinity of the surface contribute to the integral in Eq. (B.2). Hence,

$$G(t) \simeq G_0 \cdot \left[1 - \frac{1}{2v_0} \oint_{s_0} \mathrm{d}s \int_0^{\infty} \mathrm{d}h \tilde{\Phi}\left(\frac{h}{2(Dt)^{1/2}} \right) \right] = G_0 \cdot \left[1 - \frac{s_0}{v_0} \left(\frac{Dt}{\pi} \right)^{1/2} \right], \tag{B.3}$$

where s_0 is the surface of the object. This is Eq. (27) in the main body of the paper.

References

[1] R.N. Muller, P. Gillis, F. Moiny, A. Roch, Transverse relaxivity of particulate MRI contrast media: from theories to experiments, Magn. Reson. Med. 22 (1991) 178.

[2] S. Ogawa, R.S. Menon, D.W. Tank, S.-G. Kim, H. Merkle, J.M. Ellerman, K. Ugurbil, Functional brain mapping by blood oxygenation level-dependent contrast magnetic resonance imaging, Biophys. J. 64 (1993) 803.

[3] J.C. Ford, F.W. Wehrli, H.W. Chung, Magnetic field distribution in models of trabecular bone, Magn. Reson. Med. 30 (1993) 373.

[4] R.M. Weiskoff, C.S. Zuo, J.L. Boxerman, B.R. Rosen, Microscopic susceptibility variation and transverse relaxation: theory and experiment, Magn. Reson. Med. 31 (1994) 601.

[5] J.L. Boxerman, L.M. Hamberg, B.R. Rosen, R.M. Weisskoff, MR contrast due to intravascular magnetic susceptibility perturbations, Magn. Reson. Med. 34 (1995) 555.

[6] D.A. Yablonskiy, E.M. Haacke, Theory of NMR signal behavior in magnetically inhomogeneous tissues: the static dephasing regime, Magn. Reson. Med. 32 (1994) 749.

[7] V.G. Kiselev, S. Posse, Analytical theory of susceptibility induced NMR signal dephasing in a celebrovascular network, Phys. Rev. Lett. 81 (1998) 5696.

[8] V.G. Kiselev, S. Posse, Analytical model of susceptibility-induced MR signal dephasing: effect of diffusion in a microvascular network, Magn. Reson. Med. 41 (1999) 499.

[9] J.H. Jensen, R. Chandra, Strong field behaviour of the NMR signal from magnetically heterogeneous tissues, Magn. Reson. Med. 43 (2000) 226.

[10] J.H. Jensen, R. Chandra, NMR relaxation in tissues with weak magnetic inhomogeneities, Magn. Reson. Med. 44 (2000) 144.

[11] A.L. Sukstanskii, D.A. Yablonskiy, Theory of FID NMR signal dephasing induced by mesoscopic magnetic field inhomogeneities in biological systems, J. Magn. Reson. 151 (2001) 107.

[12] V.G. Kiselev, D.S. Novikov, Transverse NMR relaxation as a probe of mesoscopic structure, Phys. Rev. Lett. (2002).

[13] R.P. Kennan, J. Zhong, J.C. Gore, Intravascular susceptibility contrast mechanisms in tissues, Magn. Reson. Med. 31 (1994) 9.

[14] L.A. Stables, R.P. Kennan, J.C. Gore, Asymmetric spin-echo imaging of magnetically inhomogeneous systems: theory, experiment, and numerical studies, Magn. Reson. Med. 40 (1998) 432.

[15] P.W. Anderson, P.R. Weiss, Exchange narrowing in paramagentic resonance, Rev. Mod. Phys. 25 (1953) 269.

[16] D.C. Douglass, D.W. McCall, Diffusion in paraffin hydrocarbons, J. Phys. Chem. 62 (1958) 1102.

[17] C.H. Neuman, Spin echo of spin diffusion in a bounded medium, J. Chem. Phys. 60 (1973) 4508.

[18] P.T. Callaghan, Principles of Nuclear Magnetic Resonance Microscopy, Claredon Press, Oxford, NY, 1991.

[19] L.Z. Wang, A. Caprihan, E. Fukushima, The narrow-pulse criterion for pulsed-gradient spin-echo diffusion measurements, J. Magn. Reson. A 117 (1995) 209.

[20] J. Stepisnik, Validity limits of Gaussian approximation in cumulant expansion for diffusion attenuation of spin echo, Physica B 270 (1999) 110.

[21] A.L. Sukstanskii, D.A. Yablonskiy, Effects of restricted diffusion on MR signal formation, J. Magn. Reson. 157 (2002) 92.

[22] A.L. Sukstanskii, D.A. Yablonskiy, Theory of FID NMR signal dephasing induced by mesoscopic magnetic field inhomogeneities in biological systems, J. Magn. Reson. 151 (2001) 107.

[23] I.S. Gradstein, I.M. Ryzhik, Table of Integrals, Series, and Products, Academic Press, New York, 1999.

[24] S. Majumdar, J.C. Gore, Studies of diffusion in random fields produced by variations in susceptibility, J. Magn. Reson. 78 (1988) 41.

[25] D.W. Pfitsch, A.F. McDowell, M.S. Conradi, What are the conditions for exponential time-cubed echo decays?, J. Magn. Reson. 139 (1999) 364.

[26] A. Abragam, Principles of Nuclear Magnetism, Oxford University Press, New York, 1989.

[27] Y. Ayant, E. Belorizky, J. Alizon, J. Gallice, Calcul des densites spectrales resultant d'un mouvement aleatoire de translation en relaxation par interaction dipolaire magnetique dans les liquides, J. Phys. 36 (1975) 991.

[28] Y. Gossuin, P. Gillis, F. Lo Bue, Susceptibility-induced T(2)-shortening and unrestricted diffusion, Magn. Reson. Med. 47 (2002) 194.

[29] D.A. Yablonskiy, Quantitation of intrinsic magnetic susceptibility-related effects in a tissue matrix. Phantom study, Magn. Reson. Med. 39 (1998) 417.

[30] P.P. Mitra, P.N. Sen, L.M. Schwartz, Short-time behavior of the diffusion coefficient as a geometrical probe of porous media, Phys. Rev. B 47 (1993) 8565.

[31] S.C.-K. Chu, Y. Xu, J.A. Balschi, C.S. Springer, Bulk magnetic susceptibility shift in NMR studies of compartmentalized samples: use of paramegnetic reagents, Magn. Reson. Med. 13 (1990) 239.